

Epitaxial thin films of hexagonal BaRuO₃ on (001) SrTiO₃

M. K. Lee, C. B. Eom, J. Lettieri, I. W. Scrymgeour, D. G. Schlom, W. Tian, X. Q. Pan, P. A. Ryan, and F. Tsui

Citation: *Applied Physics Letters* **78**, 329 (2001); doi: 10.1063/1.1338965

View online: <http://dx.doi.org/10.1063/1.1338965>

View Table of Contents: <http://scitation.aip.org/content/aip/journal/apl/78/3?ver=pdfcov>

Published by the [AIP Publishing](#)

Articles you may be interested in

[Magnetic and transport properties of epitaxial \(LaBa\)Co₂O_{5.5+δ} thin films on \(001\) SrTiO₃](#)

Appl. Phys. Lett. **96**, 132106 (2010); 10.1063/1.3378877

[Magnetic properties of epitaxial Mn-doped ZnO thin films](#)

J. Appl. Phys. **93**, 7876 (2003); 10.1063/1.1556125

[Response to "Comment on 'Lattice deformation and magnetic properties in epitaxial thin films of Sr_{1-x}Ba_xRuO₃'" \[Appl. Phys. Lett. 77, 600 \(2000\)\]](#)

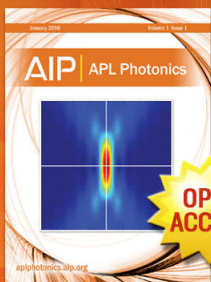
Appl. Phys. Lett. **77**, 602 (2000); 10.1063/1.127058

[Comment on "Lattice deformation and magnetic properties in epitaxial thin films of Sr_{1-x}Ba_xRuO₃" \[Appl. Phys. Lett. 73, 1200 \(1998\)\]](#)

Appl. Phys. Lett. **77**, 600 (2000); 10.1063/1.127057

[Anisotropic electrical transport in epitaxial La_{2/3}Ca_{1/3}MnO₃ thin films](#)

J. Appl. Phys. **87**, 5570 (2000); 10.1063/1.373407



Launching in 2016!

The future of applied photonics research is here

AIP | APL
Photonics

Epitaxial thin films of hexagonal BaRuO₃ on (001) SrTiO₃

M. K. Lee and C. B. Eom^{a)}

Department of Materials Science & Engineering, University of Wisconsin-Madison, Madison, Wisconsin 53706

J. Lettieri, I. W. Scrymgeour, and D. G. Schlom

Department of Materials Science and Engineering, Pennsylvania State University, University Park, Pennsylvania 16803-6602

W. Tian and X. Q. Pan

Department of Materials Science and Engineering, University of Michigan, Ann Arbor, Michigan 48109

P. A. Ryan and F. Tsui

Department of Physics and Astronomy, University of North Carolina, Chapel Hill, North Carolina 27599

(Received 6 July 2000; accepted for publication 8 November 2000)

We report the growth, epitaxial arrangement, and electrical and magnetic properties of epitaxial thin films of hexagonal BaRuO₃ on (001) cubic perovskite substrates. Four-circle x-ray diffraction reveals that the BaRuO₃ films are predominantly grown with two distinct orientations normal to the (001) SrTiO₃ substrate: (02 $\bar{2}$ 3) of the four-layered hexagonal structure (4H) in the sputter-grown films and (20 $\bar{2}$ 5) of the nine-layered hexagonal structure (9R) in the pulsed laser deposited films. (02 $\bar{2}$ 3)-oriented 4H films consist of four orthogonal domains with the in-plane relationship of BaRuO₃[2 $\bar{1}$ $\bar{1}$ 0]//SrTiO₃(110). The temperature dependent resistivity of the (02 $\bar{2}$ 3) 4H film shows metallic behavior. In contrast, a resistivity minimum is observed at low temperatures in the (20 $\bar{2}$ 5) 9R film. Both films exhibit Pauli paramagnetism. © 2001 American Institute of Physics. [DOI: 10.1063/1.1338965]

Simple ruthenium based oxides (ARuO₃:A = Ba > Sr > Ca in cation size) have received much attention owing to their interesting magnetic properties and potential for device applications. SrRuO₃ is a 4*d* itinerant ferromagnet with $T_C \sim 160$ K,¹ whereas CaRuO₃ exhibits no magnetic order,² although both have very similar pseudocubic perovskite structures.³ The striking difference between SrRuO₃ and CaRuO₃ in magnetic properties makes BaRuO₃ interesting, particularly if BaRuO₃ also has a pseudocubic perovskite structure. Bulk BaRuO₃ ceramics have been synthesized with three different crystal structures as a function of synthesis pressure.⁴ As the synthesis pressure increases, BaRuO₃ transforms to the structure containing more cubic-close packing and fewer hexagonal-close packing of BaO₃ layers; from the nine-layered rhombohedral (9R) with $a = 5.75$ Å and $c = 21.6$ Å,^{4,5} to the four-layered hexagonal (4H) with $a = 5.73$ Å and $c = 9.5$ Å,^{4,6} and finally the six-layered hexagonal (6H) with $a = 5.71$ Å and $c = 14$ Å.⁴ Much higher pressures (about 125 kbars) are expected to be necessary to form the pseudocubic polymorph of BaRuO₃, with an extrapolated lattice constant of 4.01 Å.^{4,7} It is also possible that one might be able to stabilize the pseudocubic phase by epitaxial growth using cubic perovskite substrates.

Despite our efforts to grow the desired perovskite structure, both the pulsed laser deposited (PLD) films and the sputter-grown films were not the perovskite phase, and we were unsuccessful in growing pseudocubic BaRuO₃ on (001) cubic perovskite substrates.⁷ This is in contrast to a prior report⁸ on the synthesis of tetragonal BaRuO₃ thin films on

(001) SrTiO₃ using rf sputtering techniques. However, the structural evidence presented by Fukushima *et al.*⁸ is insufficient to establish whether their films are indeed the tetragonal polymorph of BaRuO₃ or are instead the 4H or 9R polymorph.⁷

In this letter we report the growth of epitaxial thin films of hexagonal BaRuO₃ on (001) cubic perovskite substrates. We show that films containing predominantly a metastable 4H structure^{4,6} [and a minor amount of (20 $\bar{2}$ 5) 9R BaRuO₃] can be grown along a high index orientation, (02 $\bar{2}$ 3), by the 90° off-axis sputtering technique. A previous study⁷ has also shown that PLD grown films are mixed with (20 $\bar{2}$ 5) 9R and (02 $\bar{2}$ 3) 4H BaRuO₃ on the same (001) substrate. Here the electrical transport and magnetic properties of both the predominantly (02 $\bar{2}$ 3) 4H and (20 $\bar{2}$ 5) 9R films are discussed.

The films were grown on the cubic face of a variety of substrates, which include (001) LaAlO₃ ($a = 3.792$ Å), (001) SrTiO₃ ($a = 3.906$ Å), (001) KTaO₃ ($a = 3.989$ Å), (001) and (100) BaTiO₃ ($a = 3.992$ Å, $c = 4.036$ Å), and (001) MgO ($a = 4.212$ Å). The substrates, such as KTaO₃, BaTiO₃, and MgO, were used to match the extrapolated pseudocubic lattice of BaRuO₃ ($a \sim 4.01$ Å).^{4,7} The sputtering pressure was maintained at 200 mTorr with a mixture of 40% O₂ and 60% Ar. The growth temperature was varied from 550 to 750 °C, and the film thickness was between 900 and 4600 Å.

X-ray diffraction experiments reveal that except for the growths on SrTiO₃ substrates, films generally contain randomly oriented hexagonal domains of 4H BaRuO₃, such as (0001), (10 $\bar{1}$ 1), (10 $\bar{1}$ 2), and (10 $\bar{1}$ 3). Growth on (001)SrTiO₃ substrates appears to suppress the random 4H domains, as shown in the θ - 2θ pattern of Fig. 1(a). The only

^{a)}Electronic mail: eom@engr.wisc.edu

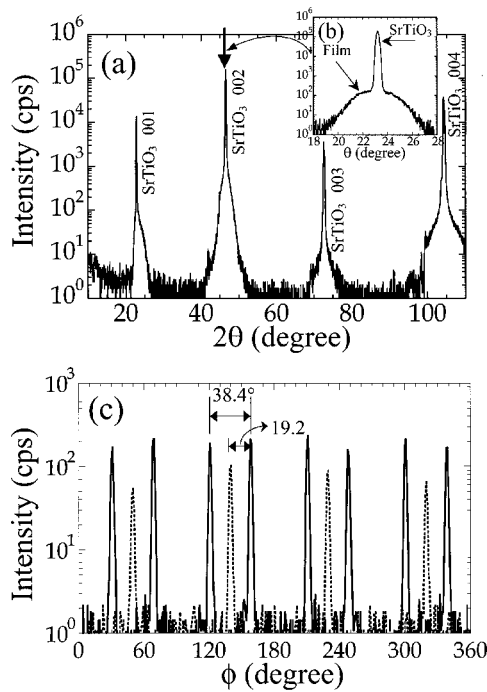


FIG. 1. (a) X-ray normal θ - 2θ diffraction pattern for the BaRuO₃ film on (001) SrTiO₃ substrate at 600 °C; (b) rocking curve measured at $2\theta = 46.50^\circ$. The arrow, “↓”, in (a) corresponds to the 02 $\bar{2}$ 3 4H reflection; (c) ϕ scan patterns of both 30 $\bar{3}$ 0 and 03 $\bar{3}$ 0 4H reflections, drawn with solid and dotted lines, respectively.

peaks observed in the θ - 2θ scans were the 001 reflections of SrTiO₃. In order to examine the overlap of the film with the substrate peaks, x-ray rocking curves were measured as a function of 2θ within the 001 peaks of SrTiO₃. The measured rocking curves show that the film peak overlaps with the 002 peak of SrTiO₃. Figure 1(b) is a typical rocking curve measured at $2\theta = 46.50^\circ$, where the broad film peak lies beneath the sharp 002 SrTiO₃ peak. The 2θ position of the film peak determined by rocking curves as a function of 2θ is consistent with either the 02 $\bar{2}$ 3 reflection of 4H structure with $2\theta = 46.50^\circ$ based on Cu $K\alpha_1$ or possibly the 002 reflection of the pseudocubic structure. However, the ϕ scans for the selected off-axis 4H reflections, such as 30 $\bar{3}$ 0 and 03 $\bar{3}$ 0, 10 $\bar{1}$ 2 and 01 $\bar{1}$ 2, and 20 $\bar{2}$ 2 and 02 $\bar{2}$ 2, confirm the predominant growth of (02 $\bar{2}$ 3) 4H phase parallel to the substrate,⁹ which is also observed in the films grown on other perovskite substrates. Among them, both 30 $\bar{3}$ 0 and 03 $\bar{3}$ 0 4H reflections are shown in Fig. 1(c). Moreover, these studies are in agreement with the TEM observations of the same BaRuO₃ films that showed the 4H structure.¹⁰

The sputter-grown 4H films contained minor amounts of (20 $\bar{2}$ 5)-oriented 9R BaRuO₃. The 9R content varied slightly with growth temperature. In the low temperature grown films (below 650 °C), the amount of (20 $\bar{2}$ 5) 9R phase was below the x-ray background level. The PLD films also show predominantly (20 $\bar{2}$ 5)-oriented 9R phase (~98%) with a slight content (~2%) of (02 $\bar{2}$ 3) 4H phase, based on an approximate calculation of the volume fraction of two polymorphs.¹¹

The surface morphology of both sputtered and PLDBaRuO₃ films was examined using scanning tunneling microscopy (STM). Figure 2(a) shows a STM image of the (02 $\bar{2}$ 3)-oriented 4H BaRuO₃ film. Surfaces exhibit nearly orthogonal long islands aligned along the $\langle 110 \rangle$ directions of

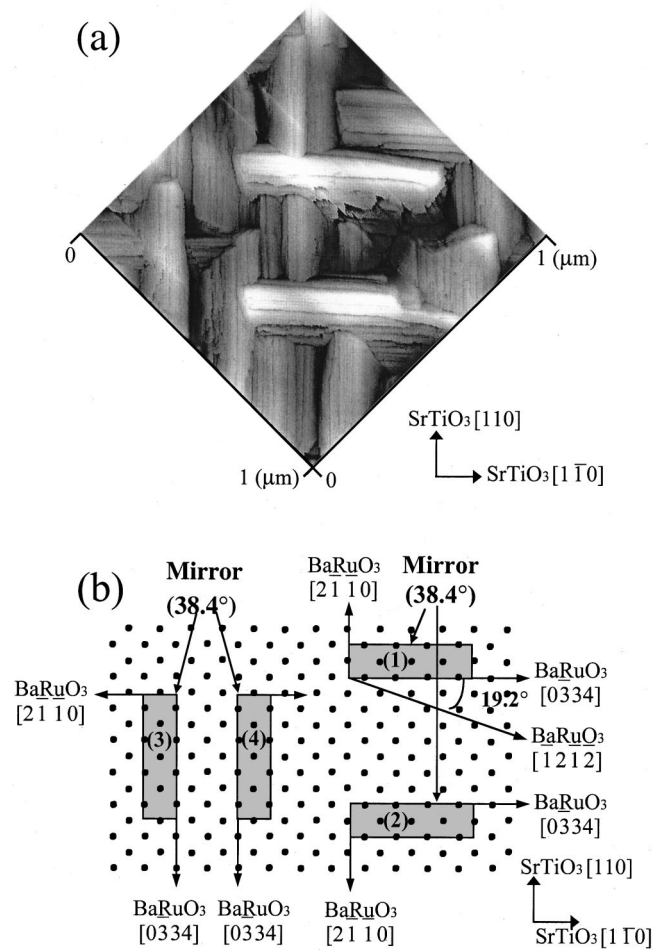


FIG. 2. (a) STM image showing nearly orthogonal domains; (b) schematic drawing of the expected domain structure and epitaxial relation from Fig. 1(c), where the rectangles indicate four (02 $\bar{2}$ 3) domains with respect to (001) surface mesh of SrTiO₃ substrate (dots).

the (001) SrTiO₃ substrate. We note that the PLD (20 $\bar{2}$ 5)-oriented 9R films also exhibit similar surface features.

The in-plane domain structures of the (02 $\bar{2}$ 3)-oriented 4H films grown on (001) SrTiO₃ substrate were determined from Fig. 1(c). The ϕ scans indicate that the (02 $\bar{2}$ 3)-oriented 4H films contain four domains in the plane; they are shown schematically in Fig. 2(b). The in-plane epitaxial relationships for the four domains confirmed by x-ray diffraction are:

$$(1) \text{BaRuO}_3[2\bar{1}\bar{1}0] \parallel \text{SrTiO}_3[110],$$

$$(2) \text{BaRuO}_3[2\bar{1}\bar{1}0] \parallel \text{SrTiO}_3[\bar{1}\bar{1}0],$$

$$(3) \text{BaRuO}_3[2\bar{1}\bar{1}0] \parallel \text{SrTiO}_3[\bar{1}10],$$

and

$$(4) \text{BaRuO}_3[2\bar{1}\bar{1}0] \parallel \text{SrTiO}_3[1\bar{1}0].$$

The domains (1) and (2) and the domains (3) and (4) are “mirror planes” with respect to each other. The in-plane tilt angle for the domains with respect to the mirror axis, as it is determined from the ϕ scans, is $\sim 19.2^\circ$, which is nearly the same as the angle ($\sim 19.6^\circ$) between the [0 $\bar{3}$ 34] and [$\bar{1}$ 2 $\bar{1}$ 2] directions in the (02 $\bar{2}$ 3) plane. These results are consistent with TEM studies of the same BaRuO₃ films.¹⁰

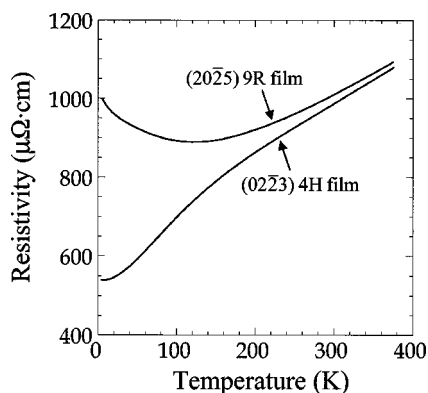


FIG. 3. Temperature dependence of electrical resistivities for both (0223) 4H and (2025) 9R BaRuO₃ thin films grown on (001) SrTiO₃ substrates.

Epitaxial match of (0223) 4H BaRuO₃ with a (001) SrTiO₃ substrate is believed to be due to the Ba–O subcells in the (0223) 4H plane (not shown here). The Ba–O subcell is nearly matched with the (001) plane of the perovskite crystal in both lattice structure and spacing with an edge spacing of ~ 4.1 Å and corner angles of either $\sim 89^\circ$ or $\sim 91^\circ$. The diagonals ($[2\bar{1}\bar{1}0]$ or $[0\bar{3}34]$) of the Ba–O subcell can be thus matched to the 110 directions of the perovskite substrate, which allows four possible (0223) domains.

Electrical transport properties of the predominantly (0223)-oriented 4H films have been studied along with those of the predominantly (2025)-oriented 9R films using four terminal techniques in a temperature range between 4.2 and 380 K. As shown in Fig. 3, the resistivity values at 300 K are about 990 and 1010 $\mu\Omega$ cm for the 4H and 9R phases, respectively. These two films show quite different temperature-dependent behavior. The (0223)-oriented 4H film maintains metallic behavior over the whole range of temperature, such that the temperature dependent resistivity is almost linear with just a slight curvature at low temperatures. The behavior at high temperatures appears to be more linear than that of the (0001)-oriented 4H films reported elsewhere.¹² The dependence below 45 K is nearly quadratic. A T^2 fit in this temperature range gives a residual resistivity of 540 $\mu\Omega$ cm. The observed room temperature and residual resistivities are higher than those of single domain (0001)-oriented 4H films, which can be attributed to the presence of four in-plane domains leading to enhanced domain boundary scattering. In contrast to the behavior of the predominantly (0223)-oriented 4H film, the resistivity of the predominantly (2025)-oriented 9R film shows metallic behavior at high temperatures but exhibits a broad minimum around 140 K before rising to a more resistive state as the temperature decreases. This behavior is similar to those of 9R single crystals.¹³

Magnetic properties have also been measured as a function of temperature from 5 to 400 K by SQUID magnetometry. Both the predominantly (0223)-oriented 4H and the (2025)-oriented 9R films exhibit paramagnetism; the magnetic volume susceptibility is less than 5×10^{-5} emu/cm³ and is nearly temperature independent, indicating that it is

dominated by Pauli paramagnetism. This finding is totally different from the reported observation of ferromagnetism with T_C of ~ 50 K in films of the “cubic” BaRuO₃ polymorph by Fukushima *et al.*⁸ However, it is comparable to those observed in bulk 9R and 4H single crystals¹³ and in the (0001)-oriented 4H epitaxial thin film.¹² We believe that the reported ferromagnetism may be attributed to impurities in the sample.

In conclusion, we have studied the epitaxial growth and properties of hexagonal BaRuO₃ on (001) cubic perovskite substrates. The most favorable growth parallel to the substrates was found to be the (0223) plane in 4H BaRuO₃ and the (2025) plane in 9R BaRuO₃ with four in-plane domains. The temperature-dependent resistivity of the predominantly (0223)-oriented 4H film shows metallic behavior, and it is slightly curved at low temperatures. Its predominantly (2025)-oriented 9R counterpart exhibits a minimum around 140 K. Pauli paramagnetism dominates the magnetic properties of the two phases. Electrical transport and magnetic properties of the two crystallographic forms grown by the epitaxial processes are comparable to those of bulk single crystals.

The authors would like to thank Bob Cava for helpful discussions. This work was supported by NSF Grant Nos. DMR-980244, DMR-9973801, a NSF Young Investigator Award (C.B.E.), a David and Lucile Packard Fellowship (C.B.E.), College of Engineering at the University of Michigan (X.Q.P.), NSF DMR-9703419 (F.T.), and NSF DMR-9601825 (F.T.).

- ¹A. Callaghan, C. W. Moeller, and R. Ward, *Inorg. Chem.* **5**, 1572 (1966).
- ²T. C. Gibb, R. Greatrex, N. N. Greenwood, and P. Kaspi, *J. Chem. Soc. Dalton Trans.* **1973**, 1253 (1973).
- ³H. Kobayashi, M. Nagata, R. Kanno, and Y. Kawamoto, *Mater. Res. Bull.* **29**, 1271 (1994).
- ⁴J. M. Longo and J. A. Kafalas, *Mater. Res. Bull.* **3**, 687 (1968).
- ⁵P. C. Donohue, L. Katz, and R. Ward, *Inorg. Chem.* **4**, 306 (1965).
- ⁶S. T. Hong and A. W. Sleight, *J. Solid State Chem.* **128**, 251 (1997).
- ⁷J. Lettieri, I. W. Scrymgeour, D. G. Schlom, M. K. Lee, and C. B. Eom, *Appl. Phys. Lett.* **77**, 600 (2000).
- ⁸N. Fukushima, K. Sano, T. Schimizu, K. Abe, and S. Komatsu, *Appl. Phys. Lett.* **73**, 1200 (1998).
- ⁹Off-axis ϕ scans were carried out to determine the rotation ϕ relationship in the (0223) plane between the selected off-axis 4H reflections: 3030 and 0330, 1012 and 0112, and 2022 and 0222. The calculated ϕ angles between the planes based on 4H single crystal (Ref. 6) were 109.6° (or 70.4°), 121° (or 59°), and 97° (or 83°) in that order. These values were compared with the measured ones. This work makes the (0223) 4H phase distinguishable from other polymorphs such as 9R or pseudocubic.
- ¹⁰W. Tian, X. Q. Pan, M. K. Lee, and C. B. Eom, *Appl. Phys. Lett.* **77**, 1985 (2000).
- ¹¹Integrated intensities and other factors (formula units of the respective unit cells, structure and multiplicity factors) of 0115_{9R} and 1012_{4H} reflections were considered to determine the volume fractions of the (2025)_{9R} and (0223)_{4H} normal orientations in the films. The Lorentz polarization and geometrical factors were neglected because the θ and χ values of both reflections are very close to each other. The absorption and temperature factors were assumed to be equal. The measured peak widths for both 0115_{9R} and 1012_{4H} reflections were also found to be comparable.
- ¹²M. K. Lee, C. B. Eom, W. Tian, X. Q. Pan, M. Smoak, F. Tsui, and J. J. Krajewski, *Appl. Phys. Lett.* **77**, 364 (2000).
- ¹³J. T. Rijssenbeek, R. Jin, Y. Zadorozhny, Y. Liu, B. Batlogg, and R. J. Cava, *Phys. Rev. B* **59**, 4561 (1999).